Volume 303, number 2,3, 136–140 FEBS 11079 June 1992

^{15}N NMR assignments and chemical shift analysis of uniformly labeled ^{15}N calbindin D_{9k} in the apo, $(Cd^{2+})_1$ and $(Ca^{2+})_2$ states

Nicholas J. Skelton[a], Mikael Akke[a,b], Johan Kördel[a,b], Eva Thulin[b], Sture Forsén[b] and Walter J. Chazin[a]

[a]*Department of Molecular Biology, The Scripps Research Institute, La Jolla, CA 92037, USA* and [b]*Department of Physical Chemistry 2, Chemical Centre, University of Lund, S-221 00 Lund, Sweden*

Received 9 March 1992

^{15}N has been uniformly incorporated into the EF-hand Ca^{2+}-binding protein calbindin D_{9k} so that heteronuclear experiments can be used to further characterize the structure and dynamics of the apo, $(Cd^{2+})_1$ and $(Ca^{2+})_2$ states of the protein. The ^{15}N NMR resonances were assigned by 2D ^{15}N-resolved ^1H experiments, which also allowed the identification of a number of sequential and medium-range ^1H–^1H contacts that are obscured by chemical shift degeneracy in homonuclear experiments. The ^{15}N chemical shifts are analyzed with respect to correlations with protein secondary structure. In addition, the changes in ^{15}N chemical shift found for the apo→$(Cd^{2+})_1$→$(Ca^{2+})_2$ binding sequence confirm that the effects on the protein are mainly associated with chelation of the first ion.

Nuclear magnetic resonance; Protein structure; Ca^{2+}-binding protein

1. INTRODUCTION

The calcium ion is a ubiquitous 'second messenger' involved in a variety of cellular processes, including cell division and growth, muscle contraction, secretion, and certain metabolic processes [1–3]. Calcium-binding proteins play a central role in the translation of the Ca^{2+} signal, undergoing Ca^2-dependent conformational changes that modulate their interaction with other cellular components. This family of proteins is characterized by a common helix–loop–helix structural motif in their binding sites, termed the EF-hand [4]. Aside from regulatory functions, EF-hand Ca^{2+}-binding proteins are involved in transport and buffering of Ca^{2+} within the cell [5]; calbindin D_{9k} is one such example [6].

The structure of Ca^{2+}-loaded calbindin D_{9k} has been determined by X-ray crystallography [7]; the protein comprises four helices (numbered I to IV) and two calcium-binding loops arranged in two EF-hand motifs, with a nine-residue linker between them. Our research program involves determining the effects of Ca^{2+}-binding on the structure and dynamics of the protein and identifying the molecular basis for the relative affinity, ion selectivity and cooperativity in the binding of Ca^{2+} [8–10]. The assignment of the ^1H resonances and identification of the secondary structure and global folding pattern in the apo and $(Ca^{2+})_2$ states have been reported [11,12]. To address the question of the cooperativity, the $(Cd^{2+})_1$ state has also been studied [13]. Since the binding of Cd^{2+} is sequential, with the first ion entering the C-terminal EF hand [13,14], $(Cd^{2+})_1$ calbindin D_{9k} serves as a model for the thermodynamically inaccessible $(Ca^{2+})_1$ state. As part of our effort to fully characterize the structure and dynamics of calbindin D_{9k} samples of the protein enriched in ^{15}N have been prepared. This report briefly describes some of the details of the protein production, the sequence-specific assignment of the ^{15}N NMR resonances in the apo, $(Cd^{2+})_1$ and $(Ca^{2+})_2$ states, and an analysis of the ^{15}N chemical shifts for the three states of metal occupancy.

Abbreviations: NMR, nuclear magnetic resonance; 1D, one-dimensional; 2D, two-dimensional; FID, free induction decay; HSQC, heteronuclear single quantum coherence; NOE, nuclear Overhauser effect; NOESY, 2D NOE spectroscopy; TOCSY, total correlation spectroscopy; P43G, the sequence of the minor A form of bovine calbindin D_{9k} produced by recombinant DNA methodology, with an additional methionine at the N-terminus and the Pro-^{43}→Gly mutation; IPTG, isopropyl β-D-thiogalactopyranoside; RMSD, root mean square difference.

Correspondence address: W.J. Chazin, Dept. Molecular Biology (MB-2), 10666 N. Torrey Pines Road, The Scripps Research Institute, La Jolla, CA 92037, USA. Fax: (1) (619) 554-9822.

2. MATERIALS AND METHODS

The general methods utilized for synthesis of the calbindin D_{9k} gene, expression in *E. coli*, and protein purification have been reported [15,16]. The utilization of a new expression system [17] for producing ^{15}N labeled protein is described below in section 3. The (99%-$^{15}NH_4)_2SO_4$ and 99%-$^{15}NH_4Cl$ was purchased from M.S.D. Isotopes (Montréal, Canada). Decalcification and titration of the protein with Cd^{2+} were performed as described previously [13,18]. The apo, $(Cd^{2+})_1$ and $(Ca^{2+})_2$ samples were prepared from 16–20 mg of lyophilized protein, dissolved in 420 μl of 95% H_2O/5% ^2H_2O (4–5 mM) and adjusted to pH 6.0 by the addition of μl amounts of 1 M HCl or 1 M NaOH.

The NMR spectra were acquired on Bruker AMX 500 and AM 600 spectrometers, at 300 K. The H_2O peak was suppressed by low power

 Published by Elsevier Science Publishers B.V.

coherent irradiation of the water resonance for 1.2–1.5 s prior to each pulse train, or by the use of spin–lock purge pulses during the inept coherence transfer steps [19]. ^{15}N decoupling was achieved with GARP-1 phase-modulated irradiation [20]. The phase-sensitive data were obtained using the time proportional phase incrementation method for quadrature detection in the ω_1 dimension [21]. ^1H chemical shifts were referenced to the H_2O peak at 4.75 ppm, and the ^{15}N shifts referenced indirectly to liquid NH_3 by using the ^1H frequency of the H_2O resonance [22,23]. HSQC ^{15}N-^1H correlation, HSQC-NOESY and HSQC-TOCSY spectra were acquired using standard pulse sequences [24,25]. 32 or 64 transients/t_1 value were acquired with 4096 complex data points over a spectral width of 12,500 Hz in the ^1H dimension. In the ^{15}N dimension, 400 to 600 increments of t_1 were recorded with t_{1max} ranging from 110 to 150 ms. The mixing time used in the HSQC-NOESY spectra was 150 ms. HSQC-TOCSY spectra were recorded with an 80 ms DIPSI-2 spin–lock pulse train [26] at a field strength of 9.5 kHz.

NMR data were processed with the FTNMR software provided by Dr. Dennis Hare (Hare Research Inc., Woodinville, WA) and modified by Dr. Mark Rance. Artifacts arising from incompletely suppressed solvent resonances were minimized by removing the low frequency components of each FID prior to ω_2 processing [27]. The spectra were processed with gaussian or sinebell window functions to improve resolution. After the ω_2 transform, the rows of data were baseline-corrected by a simple two-point spline routine to remove linear offsets. For the analysis of chemical shifts, sinusoidal curve fitting was performed using TEMPLEGRAPH (Mihalisin Associates, Temple University, Ambler, PA 19002), the amplitude, offset, phase and period were initially adjusted manually for a best fit, then refined using non-linear least squares fitting.

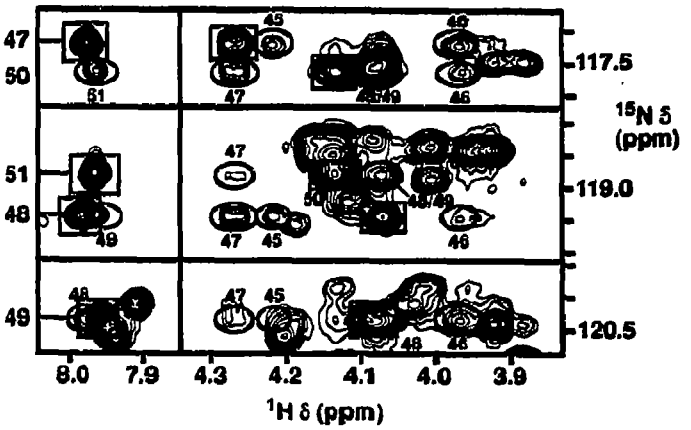

Fig. 1. Sections of the 600 MHz 2D HSQC-NOESY spectrum of apo calbindin D_{9k} acquired at pH 6.0 and 300 K, with a mixing time of 150 ms, depicting NOEs involving the amide protons of residues Asp-^{47}, Glu-^{48}, Leu-^{49}, Phe-^{50} and Glu-^{51}. Sequential d_{NN} cross peaks and ^{15}N-^1H autocorrelation peaks are shown in the left panel and intra-residue, sequential and medium range $d_{\alpha N}$ cross peaks are shown in the right panel. Boxes are drawn around the intra-residue peaks, and the sequential and medium range peaks are circled. The NOEs between protons in residue i and residue j are identified by the labels along the left hand axis (corresponding to the resonance position of the ^{15}N attached to amide proton in residue i) and the labels adjacent to the circles (corresponding to residue j). In the left panel the contours are drawn at eight-times higher intensities than in the right panel. The tick marks along the ^{15}N axis are drawn every 0.25 ppm.

3. RESULTS AND DISCUSSION

^{15}N-Enriched calbindin D_{9k} was expressed from an *E. coli* strain containing the plasmid pRCB [17]. In addition to the calbindin D_{9k} gene, the *tac* promoter, and the *lacIQ* gene, the pRCB plasmid contained a temperature-sensitive mutation in the copy number control region. With this heat- and IPTG-inducible expression system, the total *E. coli* protein expression was 5–10-fold higher than the originally reported expression system [15]. The bacteria were grown in a variation of M9 media [28], using 1.0 g/l (99%-$^{15}NH_4)_2SO_4$ or 0.75 g/l 99%-$^{15}NH_4Cl$ as the sole nitrogen source. The only modification to this protocol was that tap water, rather than distilled water, was used to prepare the media since this was found to almost double the yield of calbindin D_{9k}. Subsequent protein purification followed the procedure described in Chazin et al. [29], resulting in 30–40 mg of uniformly ^{15}N-labeled calbindin D_{9k} per litre of medium, or 50–70% of the yield obtained with nutrient-rich broth. Examination of resolved amide proton resonances by 1D ^1H NMR revealed that ^{15}N had been incorporated to greater than 95% atom.

In general, the ^{15}N-^1H correlation spectra of apo, $(Cd^{2+})_1$ and $(Ca^{2+})_2$ calbindin D_{9k} were well resolved. Many of the ^{15}N resonances could be assigned directly in these spectra because the ^1H chemical shifts of the corresponding amide protons are unique [11–13]. The sequence-specific assignments for most of the remaining ^{15}N resonances were readily obtained from the relayed peaks observed in the HSQC-TOCSY by matching backbone and sidechain connectivities to the known ^1H chemical shifts. Severe resonance overlap was observed only for Lys-^{41}/Lys-^{55} and Leu-^{28}/Ser-^{62} in the apo state, Phe-^{66}/Leu-^{32} and Leu-^{39}/Ile-^{9} in the $(Cd^{2+})_1$ state, and Glu-^{26}/Ser-^{44} in the $(Ca^{2+})_2$ state. In these few cases of extreme resonance degeneracy the assignments were made from sequential NOEs in the HSQC-NOESY spectrum. The complete list of ^{15}N assignments for all three states of the protein is given in Table I.

The HSQC-NOESY spectrum also provides a powerful method for clarification of ambiguities in ^1H chemi-

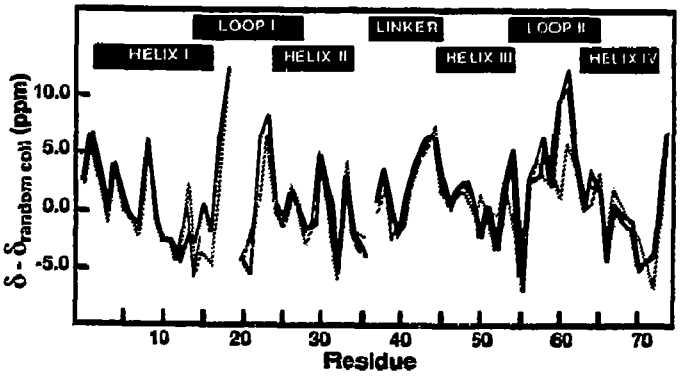

Fig. 2. Variation in the ^{15}N chemical shifts of the backbone amides in the apo, $(Cd^{2+})_1$ and $(Ca^{2+})_2$ states of calbindin D_{9k}. The observed ^{15}N chemical shifts, adjusted by subtracting the random-coil shifts [30,31]. The data are drawn with a dashed line for the apo state, with a thin solid line for the $(Cd^{2+})_1$ state and with a thick solid line for the $(Ca^{2+})_2$ state.

cal shift and NOESY cross-peak assignments. An example is shown in Fig. 1 for helix III of apo calbindin D_{9k}, where there are assignment problems in the ^1H spectrum caused by overlap of the amide protons of Asp-[47], Glu-[48], Leu-[49] and Glu-[51] [11]. The corresponding ^{15}N chemical shifts of these residues are seen to be well dispersed in the HSQC-NOESY spectrum, allowing the identification of a number of previously unassigned sequential and medium-range d_{NN} and $d_{\alpha N}$ NOEs. We have found the HSQC-NOESY spectra to be extremely valuable for identifying additonal NOEs, with in excess of 100 found for both the apo the Ca^{2+}-loaded states (the analysis for the $(Cd^{2+})_1$ state is still in progress).

The ^{15}N resonance assignments provide an opportunity to search for correlations between ^{15}N chemical shifts and structural elements of the protein, and to analyze the response of the ^{15}N chemical shift to ion binding. Studies by Glushka et al. [30] have shown that the ^{15}N chemical shift in peptides are dominated by the identity of the adjacent residues; consequently, to detect other influences, the chemical shifts have to be plotted as the secondary shift, the observed experimental values minus the random coil shifts [30,31]. The most striking feature in the plots of the backbone ^{15}N resonances secondary shifts of calbindin D_{9k} (Fig. 2) is the similarity of the profiles for each of the helical regions in the three metal-bound states, which indicates that there are no substantial changes in the local backbone conformation of the helices in response to ion binding. These results, and similar analyses of amide ^1H chemical shifts [11,13], confirm earlier conclusions about the overall similarity of the apo, (Cd^{2+}) and $(Ca^{2+})_2$ states [18]. Note that in the present study, the data were collected under identical conditions for all three states of the protein, thereby removing any possible uncertainty due to the small differences in pH [13] or structure (wild-type vs. Pro-[43]→Gly mutant) [13], as in the earlier studies.

The ^{15}N chemical shifts have been further analyzed by the method of Kuntz and co-workers [32] who reported that the variation of ^1H chemical shift is periodic in a series of helical peptides and in helical segments of protein, and that ^{15}N chemical shifts also exhibit periodicity in helices, although the latter was based on a limited data set. Periodicity is readily identified in the ^1H chemical shifts in helices I, II and III in all three states of calbindin D_{9k} (eg. Fig. 3), but not in helix IV. The periodicities derived from non-linear regression analysis are all between 3 and 4 residues per cycle (Table II), paralleling the structural periodicity of helices. However, there is no correlation apparent between the value

Table 1

^{15}N chemical shifts of calbindin D_{9k} at pH 6.0, 300 K[a]

	Ca2	Cd1	Apo		Ca2	Cd1	Apo		Ca2	Cd1	Apo
Lys[b]	123.55	123.67	nd	Glu[27]	119.84	119.09	119.96	Leu[53]	115.38	115.57	118.59
Ser[2]	119.11	118.99	119.04	Leu[28]	118.94	119.57	120.35	Asp[54]	117.62	117.86	118.85
Glu[4]	117.62	117.40	116.82	Lys[29]	119.62	119.21	118.50	Lys[55]	126.49	126.29	120.20
Glu[5]	121.76	121.62	121.77	Leu[30]	118.00	118.03	118.81	Asn[56]	111.86	113.21	116.50
Leu[6]	120.05	119.86	119.15	Leu[31]	123.86	123.86	124.31	Asn[56]N	113.52	112.82	112.75
Lys[7]	120.68	120.63	120.79	Leu[32]	119.59	119.84	120.39	Gly[57]	108.87	109.16	108.58
Gly[8]	105.01	105.04	104.87	Gln[33]	114.05	114.12	113.76	Asp[58]	118.51	119.38	119.94
Ile[9]	122.49	122.41	121.64	Gln[33]N	110.05	110.18	110.08	Gly[59]	112.85	112.65	109.25
Phe[10]	119.96	119.69	119.68	Thr[34]	110.46	110.77	112.30	Glu[60]	117.88	118.27	118.65
Glu[11]	115.04	115.21	115.63	Glu[35]	115.88	116.05	116.26	Val[61]	126.25	126.29	118.22
Lys[12]	118.73	118.56	118.41	Phe[36]	114.34	114.51	115.95	Ser[62]	126.46	124.85	120.35
Tyr[13]	114.75	114.82	115.39	Ser[38]	113.54	113.45	112.95	Phe[63]	122.92	122.68	122.14
Ala[14]	118.97	121.57	123.94	Leu[39]	122.46	122.46	120.98	Glu[64]	118.15	118.03	118.17
Ala[15]	116.77	113.76	114.19	Leu[40]	116.68	116.75	118.35	Glu[65]	120.99	119.93	118.68
Lys[16]	119.86	116.80	115.82	Lys[41]	119.93	119.93	120.26	Phe[66]	119.38	119.76	121.40
Glu[17]	115.81	nd	113.41	Gly[42]	108.51	108.15	108.60	Gln[67]	115.09	115.21	116.70
Gly[18]	112.87	109.23	108.21	Gly[43]	109.70	108.60	109.10	Gln[67]N	111.34	110.98	110.23
Asp[19]	127.69	126.10	126.36	Ser[44]	117.06	116.94	116.37	Val[68]	117.35	116.94	118.85
Asn[21]	114.51	114.65	114.87	Thr[45]	113.67	113.86	115.11	Leu[69]	120.05	119.91	120.90
Asn[21]N	114.33	114.89	115.09	Leu[46]	122.15	122.08	122.09	Val[70]	116.17	115.33	115.82
Gln[22]	113.95	116.58	117.48	Asp[47]	116.68	116.82	117.39	Lys[71]	117.67	118.03	120.53
Gln[22]N	109.62	106.34	119.38	Glu[48]	119.33	119.38	119.15	Lys[72]	116.77	116.73	116.77
Leu[23]	125.38	120.27	120.33	Leu[49]	121.52	121.35	120.66	Ile[73]	114.29	114.48	111.51
Ser[24]	120.87	nd	119.31	Phe[50]	119.02	118.97	117.61	Ser[74]	117.04	117.38	116.41
Lys[25]	121.79	122.20	121.27	Glu[51]	115.42	115.35	119.18	Gln[75]	125.98	126.10	125.90
Glu[26]	116.94	116.65	116.78	Glu[52]	118.05	117.96	117.65	Gln[75]N	111.66	111.77	111.89

[a]Chemical shifts are referenced to liquid ammonia as described in Section 2 and are accurate to ± 0.04 ppm. The side chain amides are identified by the listings with N after the residue number. The resonance for which a chemical shift could not be determined are labeled nd.

[b]The expression protocol results in an N-terminial methionine which is not cleaved from the protein (designated Met[0]), hence residues 1–75 all contain secondary amide groups. The resonances for Lys[1] in the $(Ca^{2+})_2$ and $(Cd^{2+})_1$ state were only observed in HSQC correlation spectra acquired without presuration of the water resonance.

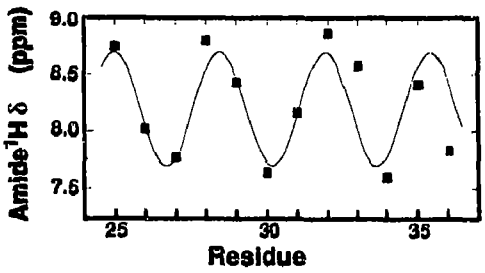

Fig. 3. Plots of ^{1}H chemical shift against residue number for helix II of $(Ca^{2+})_2$ calbindin D_{9k}. The curve represents a sinusoid calculated from a non-linear fit to the data of an equation of the form $y = A + B\ sin(Cx + D)$, where the parameters to be optimized (A, B, C, D) represent the offset, amplitude, frequency and phase, respectively. The experimental data points are indicated by filled squares. The amplitudes and periodicities resulting from the fits of the four helices are listed in Table II.

Table II

Amplitudes and periodicities of the amide proton chemical shifts observed in $(Ca^{2+})_2$, $(Cd^{2+})_1$ and apo calbindin D_{9k}

	Helix I		Helix II		Helix III		Helix IV[a]	
	A (ppm)	P (res)	A (ppm)	P (res)	A (ppm)	P (res)	A (ppm)	P (res)
Apo	0.60	3.81	0.62	3.24	0.23	3.49	0.53	3.41
$(Cd^{2+})_1$	0.37	3.84	0.56	3.37	0.54	3.95	nd	nd
$(Ca^{2+})_2$	0.37	3.72	0.50	3.47	0.54	3.92	nd	nd

[a]Helices for which no periodicity was observed are denoted by nd. Note that in the crystal structure of $(Ca^{2+})_2$ calbindin D_{9k} residues Ala[14]–Lys[16], Lys[25]–Glu[27], Asp[54]–Lys[55] and Phe[63]–Glu[65], are in both helices and binding loops. For the purposes of calculating the chemical shift RMSDs, we have included these residues only in the loop sections.

of the chemical shift and the relative surface/interior location of the residue. The absence of periodicity in helix IV probably reflects the non-uniform nature of the hydrogen-bonding pattern, compounded by fraying at the C-terminus. Having firmly established the periodic pattern of the ^{1}H chemical shift of calbindin D_{9k}, we proceeded to the corresponding analysis of the ^{15}N chemical shifts. After extensive efforts at curve fitting both the observed and secondary chemical shifts, a periodic pattern could only be detected for helix II. These results imply that the ^{15}N chemical shift may prove to be less informative than Kuntz and co-workers had anticipated.

The comparisons of pairwise RMSD of ^{15}N and ^{1}H chemical shifts between the three states of the protein (Fig. 4) provide insights into the structural and dynamical consequences of ion binding, as summarized in the following. (i) The magnitude of the chemical shift differences between the three states is greatest in the binding loops, which implies that the largest structural and/or dynamical changes in the protein induced by ion binding occur in the binding loops. (ii) The chemical shift differences of the residues in the N-terminal loop are greater when an ion binds in that site, than when an ion binds in the C-terminal site, and the converse is true for the residues in the C-terminal loop; as expected the direct effect of ion binding is greater than the effect induced by binding in the other site. (iii) The magnitudes of the chemical shift changes associated with apo→$(Cd^{2+})_1$ are larger than those associated with $(Cd^{2+})_1$→$(Ca^{2+})_2$; for the binding sequence in which the ion first binds in the C-terminal site, binding of the first ion induces a larger proportion of the structural and/or dynamical changes than binding of the second ion. (iv) The first ion-binding step induces appreciable chemical shift changes in all parts of the protein, whereas the changes associated with the second step are localized to the binding loops only. This observation is fully consistent with the previous analysis of this system by ^{1}H NMR and has important implications for the molecular basis for the cooperativity of Ca^{2+}-binding in calbindin D_{9k}, as discussed in [13].

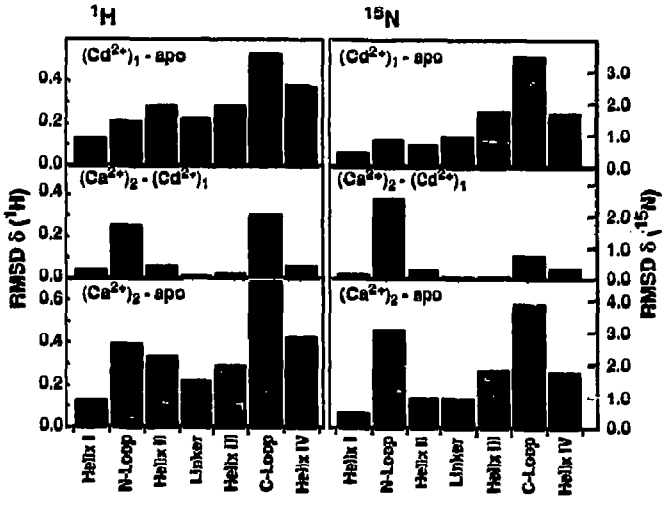

Fig. 4. Pairwise RMSD of ^{1}H and ^{15}N chemical shift between the apo, $(Cd^{2+})_1$ and $(Ca^{2+})_2$ states of calbindin D_{9k}. The protein is divided into seven structural elements as follows: Ser[-2]–Tyr[13] (helix I), Ala[14]–Glu[27] (N-loop), Leu[28]–Glu[35] (helix II), Phe[36]–Ser[44] (linker), Thr[45]–Leu[53] (helix III), Asp[54]–Glu[65] (C-loop) and Phe[66]–Ser[74] (helix IV).

The availability of the ^{15}N chemical shift assignments now sets the stage for a series of multi-dimensional heteronuclear NMR experiments to clarify ^{1}H spectral ambiguities, obtain additional distance and dihedral angle constraints for structure calculations, and to accurately measure amide proton exchange rates and ^{15}N relaxation parameters. These data will allow for a more complete characterization of the consequences of Ca^{2+}-binding on the structure and dynamics of calbindin D_{9k} than that which is possible by homonuclear ^{1}H NMR alone.

Acknowledgements: We thank Dr. Mark Rance and Dr. Arthur G. Palmer III for continued support with experimental methods, and Dr. Lawrence MacIntosh for providing a detailed description of his expression and growth procedures prior to publication. This work was

supported by the National Institutes of Health (Grant GM 40120 to W.J.C.), the American Cancer Society (fellowship JFRA-294 to W.J.C.), and the Swedish Natural Science Research Council (graduate fellowships to J.K., M.A.).

REFERENCES

[1] Rasmussen, H. (1986) New Engl. J. Med. 314, 1094–1101.
[2] Rasmussen, H. (1986) New Engl. J. Med. 314, 1164–1170.
[3] Rasmussen, H. (1989) Sci. Am. 261, 66–73.
[4] Kretsinger, R.H. (1972) Nature New Biol. 240, 85–88.
[5] Da Silva, A.C.R. and Reinach, F.C. (1991) Trends Biochem. Sci. 16, 53–57.
[6] Christakos, S., Gabrielides, C. and Rhoten, W.B. (1989) Endocr. Rev. 10, 3–26.
[7] Szebenyi, D.M.E. and Moffat, K. (1986) J. Biol. Chem. 261, 8761–8777.
[8] Forsén, S., Vogel, H. and Drakenberg, T. (1986) in: Calcium and Cell Function, vol. 6 (Cheung, W.Y., ed.) pp. 113–157, Academic Press, New York.
[9] Linse, S., Brodin, P., Drakenberg, T., Thulin, E., Sellers, P., Elmdén, K., Grundström, T. and Forsén, S. (1987) Biochemistry 26, 6723–6735.
[10] Williams, T.C., Corson, D.C., Sykes, B.D. and MacManus, J.P. (1987) J. Biol. Chem. 262, 6248–6256.
[11] Skelton, N.J., Forsén, S. and Chazin, W.J. (1990) Biochemistry 29, 5752–5761.
[12] Kördel, J., Forsén, S. and Chazin, W.J. (1989) Biochemistry 28, 7065–7074.
[13] Akke, M., Forsén, S. and Chazin, W.J. (1991) J. Mol. Biol. 220, 173–189.
[14] Vogel, H. and Forsén, S. (1987) in: Biological Magnetic Resonance, vol. 7 (Berliner, L.J. and Reuben, J., eds.) pp. 249–309, Plenum, New York.
[15] Brodin, P., Grundström, T., Hofmann, T., Drakenberg, T., Thulin, E. and Forsén, S. (1986) Biochemistry 25, 5371–5377.
[16] Chazin, W.J., Kördel, J., Drakenberg, T., Thulin, E., Hofmann, T. and Forsén, S. (1989) Biochemistry 28, 8646–8653.
[17] Brodin, P., Drakenberg, T., Thulin, E., Forsén, S. and Grundström, T. (1989) Prot. Eng. 2, 353–358.
[18] Skelton, N.J., Kördel, J., Forsén, S. and Chazin, W.J. (1990) J. Mol. Biol. 213, 593–598.
[19] Messerle, B.A., Wider, G., Otting, G., Weber, C. and Wüthrich, K. (1989) J. Magn. Reson. 85, 608–613.
[20] Shaka, A.J., Barker, P.B. and Freeman, R. (1985) J. Magn. Reson. 64, 547–552.
[21] Marion, D. and Wüthrich, K. (1983) Biochem. Biophys. Res. Commun. 113, 967–974.
[22] Live, D.H., Harris, D.G., Agosta, W.C. and Cowburn, D. (1984) J. Am. Chem. Soc. 106, 1939–1941.
[23] Bax, A. and Subramanian, S.J. (1986) J. Magn. Reson. 67, 565–569.
[24] Norwood, T.J., Boyd, J., Heritage, J.E., Soffe, N. and Campbell, I.D. (1990) J. Magn. Reson. 87, 488–501.
[25] Bax, A., Ikura, M., Kay, L.E., Torchia, D.A. and Tschudin, R. (1990) J. Magn. Reson. 86, 304–318.
[26] Shaka, A.J., Lee, C.J. and Pines, A. (1988) J. Magn. Reson. 77, 274–293.
[27] Marion, D., Ikura, M., Tschudin, R. and Bax, A. (1989) J. Magn. Reson. 85, 393–399.
[28] McIntosh, L.P. and Dalquist, F.W. (1990) Quart. Rev. Biophys. 23, 1–38.
[29] Chazin, W.J., Kördel, J., Drakenberg, T., Thulin, E., Brodin, P., Grundström, T. and Forsén, S. (1989) Proc. Natl. Acad. Sci. USA 86, 2195–2198.
[30] Glushka, L.L., Lee, M., Coffin, S. and Cowburn, D. (1989) J. Am. Chem. Soc. 111, 7716–7722.
[31] Glushka, L.L., Lee, M., Coffin, S. and Cowburn, D. (1990) J. Am. Chem. Soc. 112, 2843.
[32] Kuntz, I.D., Kosen, S. and Craig, E.C. (1991) J. Am. Chem. Soc. 113, 1406–1408.